ResearchGate

See discussions, stats, and author profiles for this publication at: https://www.researchgate.net/publication/5603970

# Ligand-Specific Changes in M 3 Muscarinic Acetylcholine Receptor Structure Detected by a Disulfide Scanning Strategy †

**ARTICLE** *in* BIOCHEMISTRY · APRIL 2008

Impact Factor: 3.02 · DOI: 10.1021/bi7019113 · Source: PubMed

CITATIONS
12

READS
33

**7 AUTHORS**, INCLUDING:

Fadi F Hamdan
CHU Sainte-Justine
**88** PUBLICATIONS **2,856** CITATIONS
SEE PROFILE

Soo-Kyung Kim
California Institute of Technology
**62** PUBLICATIONS **1,977** CITATIONS
SEE PROFILE

Kenneth A. Jacobson
National Institutes of Health
**757** PUBLICATIONS **30,460** CITATIONS
SEE PROFILE

Sung-Jun Han
Molecular Devices, LLC.
**46** PUBLICATIONS **1,306** CITATIONS
SEE PROFILE

All in-text references underlined in blue are linked to publications on ResearchGate, letting you access and read them immediately.

Available from: Sung-Jun Han
Retrieved on: 26 January 2016

# Ligand-Specific Changes in $M_3$ Muscarinic Acetylcholine Receptor Structure Detected by a Disulfide Scanning Strategy†

Jian Hua Li,‡ Fadi F. Hamdan,‡,§ Soo-Kyung Kim,|| Kenneth A. Jacobson,|| Xiaohong Zhang,‡ Sung-Jun Han,‡,⊥ and Jürgen Wess*,‡

*Molecular Signaling and Molecular Recognition Sections, Laboratory of Bioorganic Chemistry, National Institute of Diabetes and Digestive and Kidney Diseases (NIDDK), 8 Center Drive, Bethesda, Maryland 20892*

*Received September 19, 2007; Revised Manuscript Received January 3, 2008*

ABSTRACT: G protein-coupled receptor (GPCR) function can be modulated by different classes of ligands including full and inverse agonists. At present, little is known about the conformational changes that agonist ligands induce in their target GPCRs. In this study, we employed an *in situ* disulfide cross-linking strategy to monitor ligand-induced structural changes in a series of cysteine (Cys)-substituted mutant $M_3$ muscarinic acetylcholine receptors. One of our goals was to study whether the cytoplasmic end of transmembrane domain V (TM V), a region known to be critically involved in receptor/G protein coupling, undergoes a major conformational change, similar to the adjacent region of TM VI. Another goal was to determine and compare the disulfide cross-linking patterns observed after treatment of the different mutant receptors with full versus inverse muscarinic agonists. Specifically, we generated 20 double Cys mutant $M_3$ receptors harboring one Cys substitution within the cytoplasmic end of TM V (L249−I253) and a second one within the cytoplasmic end of TM VI (A489−L492). These receptors were transiently expressed in COS-7 cells and subsequently characterized in pharmacological and disulfide cross-linking studies. Our cross-linking data, in conjunction with a three-dimensional model of the $M_3$ muscarinic receptor, indicate that $M_3$ receptor activation does not trigger major structural disturbances within the cytoplasmic segment of TM V, in contrast to the pronounced structural changes predicted to occur at the cytoplasmic end of TM VI. We also demonstrated that full and inverse muscarinic agonists had distinct effects on the efficiency of disulfide bond formation in specific double Cys mutant $M_3$ receptors. The present study provides novel information about the dynamic changes that accompany $M_3$ receptor activation and how the receptor conformations induced (or stabilized) by full versus inverse muscarinic agonists differ from each other at the molecular level. Because all class I GPCRs are predicted to share a similar transmembrane topology, the conclusions drawn from the present study should be of broad general relevance.

Accumulating evidence suggests that G protein-coupled receptors (GPCRs)[1] play important roles in regulating the function of most physiological processes. In agreement with this notion, the GPCR superfamily represents the largest group of cell-surface receptors found in nature (*1–5*). An extraordinarily large number of clinically useful drugs exert their therapeutic actions via stimulating or inhibiting specific classes of GPCRs (*4*).

The structural hallmark of all GPCRs is a transmembrane core formed by a bundle of seven transmembrane helices (TM I−VII; Figure 1; *1–4*). The seven TM helices are connected by alternating intra- and extracellular loops (Figure 1). During the past 2 decades, great progress has been made in identifying specific GPCR residues involved in ligand binding and G protein coupling (*1–4, 6*). In contrast, with the exception of bovine rhodopsin (see below), much less is known about how the binding of agonists or inverse agonists leads to changes in the receptor structure that regulates the efficiency of receptor/G protein interactions.

The light receptor, bovine rhodopsin, is probably the most thoroughly studied GPCR, primarily because of its abundant expression in the retina and the ease by which it can be purified with relatively high yields from cultured cells (*7*). As a result, the conformational changes involved in light-induced activation of rhodopsin have been mapped in considerable detail (*7–11*). In brief, these structural changes are predicted to involve a reorientation of the cytoplasmic end of TM VI and changes in the relative disposition of TM VI and III, along with smaller movements involving several

† This research was supported by the Intramural Research Program of the National Institutes of Health (NIH), National Institute of Diabetes and Digestive and Kidney Diseases (NIDDK).

* To whom correspondence should be addressed: Molecular Signaling Section, Laboratory of Bioorganic Chemistry, NIH−NIDDK, Building 8A, Room B1A-05, 8 Center Drive MSC 0810, Bethesda, MD 20892-0810. Telephone: 301-402-3589. Fax: 301-480-3447. E-mail: jwess@helix.nih.gov.

‡ Molecular Signaling Section.

§ Present address: Research Center, Hopital Sainte-Justine, Montreal, Quebec, Canada H3T 1C5.

|| Molecular Recognition Section.

⊥ Present address: Invertebrate Modeling Laboratory, Institut Pasteur Korea, Seoul 136-791, Korea.

[1] Abbreviations: Cu−Phen; $Cu^{II}$−(1,10-phenanthroline)$_3$; DTT, dithiothreitol; ECL, enhanced chemiluminescence; GPCR, G protein-coupled receptor; i3 loop, the third intracellular loops of GPCRs; IP, inositol monophosphate; [$^3$H]NMS, *N*-[$^3$H]M-methylscopolamine; PAGE, polyacrylamide gel electrophoresis; PI, phosphatidyl inositol; SDS, sodium dodecyl sulfate; TM, transmembrane domain.

10.1021/bi7019113 CCC: $40.75 This article not subject to U.S. Copyright. Published 2008 by the American Chemical Society
Published on Web 02/05/2008

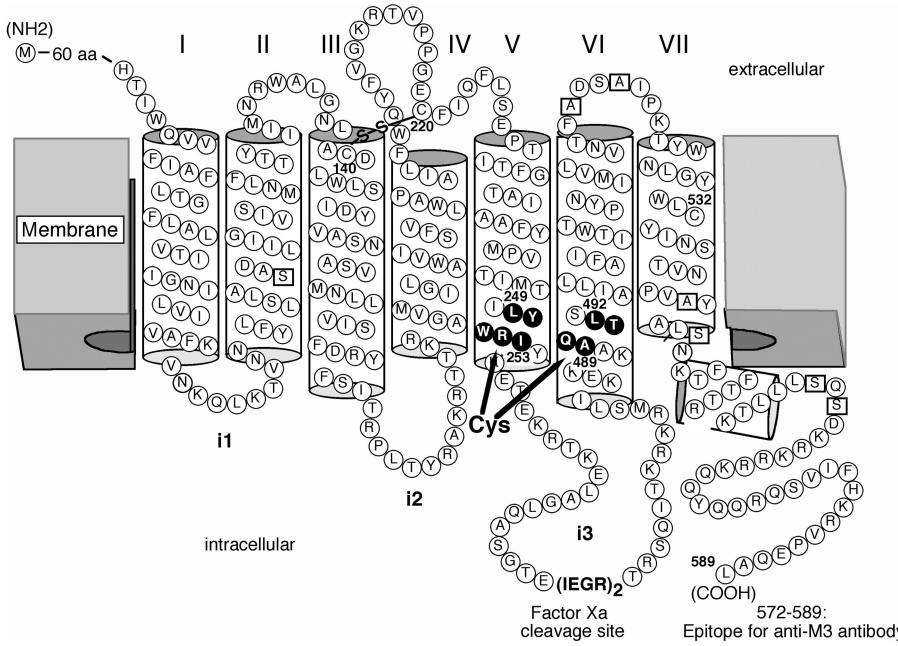


FIGURE 1: Structure of double Cys mutant $M_3$ muscarinic receptors analyzed in the present study. All Cys substitutions were introduced into a modified version of the rat $M_3$ muscarinic receptor, referred to as M3′(3C)-Xa (ref *37*). In the M3′(3C)-Xa construct, the central portion of the i3 loop (A274−K469) was replaced with two factor Xa cleavage sites. Most remaining endogenous Cys residues were replaced with either serine or alanine (open squares). The M3′(3C)-Xa construct still contained three native Cys residues, C140, C220, and C532, which proved to be essential for efficient receptor function (*37*). We generated 20 double Cys mutant receptors, all of which contained a single Cys substitution within the cytoplasmic end of TM V (L249−I253) and another one within the cytoplasmic end of TM VI (A489−L492). For Western-blotting studies, we used a rabbit polyclonal antibody (anti-M3) directly against the last 18 amino acids of the receptor protein (*38*). Numbers refer to amino acid positions in the rat $M_3$ muscarinic receptor sequence (*50*).

other TM helices (for a recent review, see ref *7*). Moreover, high-resolution structural information has been obtained for the inactive state of bovine rhodopsin via X-ray crystallography (*12, 13*).

In contrast to the rather detailed studies carried out with the light receptor, rhodopsin, relatively little is known about the structural changes involved in the activation of GPCRs that bind diffusible ligands, such as neurotransmitters and hormones. In agreement with findings obtained with bovine rhodopsin, studies with other class I (rhodopsin-like) GPCRs, including the $\beta_2$-adrenergic receptor (*14–18*) and the $M_3$ muscarinic receptor (*19, 20*), suggest that receptor activation involves an agonist-dependent rotation or reorientation of the cytoplasmic end of TM VI. Biochemical studies demonstrated that this conformational change plays a key role in receptor-mediated G protein activation (*8, 9*).

Structure–function studies with different GPCRs, including various muscarinic receptor subtypes (*21–23*), have shown that the cytoplasmic ends of TM V and VI play important roles in determining the efficiency and selectivity of receptor/G protein interactions (*6*). Whereas considerable attention has been focused on the activity-dependent conformational rearrangement of the cytoplasmic segment of TM VI, little is known about the potential structural changes that agonist ligands may induce in the cytoplasmic end of TM V.

To address this question, we used the rat $M_3$ muscarinic acetylcholine receptor, a prototypic class I GPCR (*23, 24*), as a model system. Specifically, we employed an *in situ* disulfide scanning strategy that is based on the formation of disulfide bridges between Cys residues that lie adjacent to each other in the three-dimensional (3D) structure of the receptor (*19, 20, 25–28*). This strategy does not require any receptor purification and reconstitution steps and offers the great advantage that ligand-dependent conformational changes can be studied in receptors present in their native membrane environment.

To examine whether the cytoplasmic end of TM V of the $M_3$ muscarinic receptor undergoes ligand-dependent conformational changes, we generated and analyzed a series of double Cys mutant $M_3$ receptors. Specifically, we substituted pairs of Cys residues into a mutant $M_3$ receptor (referred to as the "M3′(3C)-Xa" receptor throughout the paper) that was devoid of most native Cys residues and contained two adjacent factor Xa protease sites within the third intracellular loop (i3 loop; Figure 1). We generated 20 double Cys mutant $M_3$ receptors containing one Cys substitution within the cytoplasmic end of TM V (L249−I253) and a second one within the cytoplasmic end of TM VI (A489−L492; Figure 1 and Table 1). Because the cytoplasmic portion of TM V is located in close proximity of the corresponding region of TM VI (*12, 13*), we speculated that the TM VI Cys residues might serve as useful reporters to detect potential ligand-induced structural changes within the cytoplasmic end of TM V.

Studies with different adrenergic receptor subtypes have shown that adrenergic agonists endowed with different efficacies, including inverse agonists, induce or stabilize different receptor conformations (*29–35*). Consistent with these findings, we recently demonstrated that full muscarinic agonists and inverse muscarinic agonists had opposite structural effects on the relative orientation of helix 8 and TM I (*28*). On the basis of these findings, both full and inverse muscarinic agonists were used as ligands in the present study.

Using a disulfide scanning approach, we demonstrated that muscarinic agonists and inverse muscarinic agonists had

Table 1: Ligand Binding and Functional Properties of Double Cys Mutant $M_3$ Muscarinic Receptors Analyzed in the Present Study[a]

| | [$^3$H]-NMS binding | | carbachol binding | carbachol-induced IP production | | |
|---|---|---|---|---|---|---|
| receptor | $K_D$ (pM) | $B_{max}$ (pmol/mg of protein) | $K_i$ ($\mu$M) | $EC_{50}$ (nM) | $E_{max}$ (fold above basal) | basal IP (%) |
| M3′(3C)-Xa | 172 ± 10 | 7.4 ± 0.2 | 15.7 ± 1.6 | 24 ± 1 | 10.8 ± 0.1 | 100 |
| L249C/A489C | 179 ± 12 | 4.8 ± 1.1 | 19.1 ± 0.1 | 89 ± 8 | 20.5 ± 0.6 | 48 ± 11 |
| L249C/Q490C | 139 ± 18 | 2.3 ± 0.4 | 5.5 ± 0.8 | 3.5 ± 1.3 | 2.9 ± 0.1 | 232 ± 20 |
| L249C/T491C | 131 ± 2 | 2.4 ± 0.5 | 4.9 ± 0.8 | 77 ± 19 | 19.0 ± 0.7 | 30 ± 4 |
| L249C/L492C | 163 ± 11 | 2.2 ± 0.4 | 2.4 ± 0.1 | 24 ± 1 | 5.6 ± 0.9 | 150 ± 12 |
| Y250C/A489C | 185 ± 13 | 8.7 ± 0.5 | 2.8 ± 0.1 | 188 ± 65 | 36.9 ± 1.3 | 25 ± 5 |
| Y250C/Q490C | 169 ± 1 | 6.1 ± 0.2 | 2.2 ± 0.7 | 1.8 ± 0.4 | 3.0 ± 0.1 | 283 ± 7 |
| Y250C/T491C | 187 ± 5 | 6.0 ± 0.7 | 2.6 ± 0.3 | 121 ± 2 | 14.8 ± 0.7 | 49 ± 12 |
| Y250C/L492C | 165 ± 19 | 3.4 ± 0.1 | 1.0 ± 0.1 | 733 ± 17 | 30.5 ± 0.6 | 46 ± 11 |
| W251C/A489C | 143 ± 14 | 3.8 ± 0.3 | 6.4 ± 1.0 | 82 ± 11 | 13.5 ± 0.5 | 55 ± 12 |
| W251C/Q490C | 102 ± 1 | 1.8 ± 0.1 | 3.4 ± 0.4 | 3.8 ± 0.2 | 6.0 ± 0.9 | 257 ± 8 |
| W251C/T491C | 143 ± 13 | 2.2 ± 0.3 | 2.3 ± 0.1 | 40 ± 4 | 15.1 ± 2.4 | 48 ± 3 |
| W251C/L492C | 147 ± 11 | 1.5 ± 0.1 | 2.5 ± 0.7 | 19 ± 1 | 12.1 ± 1.3 | 249 ± 8 |
| R252C/A489C | 171 ± 34 | 5.0 ± 1.4 | 16.9 ± 0.1 | 112 ± 2 | 19.9 ± 2.4 | 82 ± 13 |
| R252C/Q490C | 171 ± 19 | 2.7 ± 0.2 | 8.0 ± 0.4 | 2.2 ± 0.5 | 2.1 ± 0.1 | 735 ± 40 |
| R252C/T491C | 178 ± 4 | 5.0 ± 0.6 | 59.3 ± 0.8 | 1680 ± 75 | 16.5 ± 1.9 | 108 ± 8 |
| R252C/L492C | 226 ± 9 | 1.9 ± 0.1 | 5.5 ± 0.3 | 28 ± 5 | 7.0 ± 0.9 | 162 ± 23 |
| I253C/A489C | 264 ± 7 | 8.9 ± 1.4 | 28.2 ± 3.4 | 70 ± 24 | 21.9 ± 2.2 | 50 ± 21 |
| I253C/Q490C | 164 ± 14 | 6.0 ± 1.0 | 11.5 ± 0.3 | 2.0 ± 0.5 | 3.0 ± 0.7 | 282 ± 21 |
| I253C/T491C | 225 ± 17 | 6.4 ± 0.9 | 6.9 ± 0.2 | 223 ± 4 | 20.1 ± 1.5 | 34 ± 1 |
| I253C/L492C | 107 ± 7 | 1.9 ± 0.1 | 0.7 ± 0.2 | 144 ± 35 | 7.2 ± 1.3 | 42 ± 1 |

[a] COS-7 cells were transiently transfected with the indicated M3′(3C)-Xa-derived double Cys mutant $M_3$ receptor constructs. Radioligand binding and PI assays were performed and analyzed as described in the Experimental Procedures. Carbachol binding data were corrected for the Cheng−Prusoff shift. Basal inositol monophosphate (IP) levels were 10 880 ± 783 dpm (=100%) for the M3′(3C)-Xa construct. Data are given as means ± standard error (SE) from at least three independent experiments, each performed in duplicate.

different effects on the efficiency of disulfide bond formation in specific double Cys mutant $M_3$ receptors. The cross-linking data, in conjunction with a 3D model of the $M_3$ muscarinic receptor, suggest that the cytoplasmic end of TM V does not undergo a major structural change, in contrast to the corresponding TM VI region. Moreover, together with a recent report (*28*), the present study provides novel information about how the receptor conformations induced (or stabilized) by full versus inverse muscarinic agonists differ from each other at the structural level.

## EXPERIMENTAL PROCEDURES

*Materials.* Acetylcholine bromide, carbamylcholine chloride (carbachol), atropine sulfate, *N*-methylscopolamine (NMS) bromide, cupric sulfate ($CuSO_4$), 1,10-phenanthroline, *N*-ethylmaleimide, digitonin, and mammalian protease inhibitor cocktail were obtained from Sigma. [$^3$H]-NMS (82.0 Ci/mmol) was from Perkin-Elmer Life Sciences, and *myo*[$^3$H]inositol (20 Ci/mmol) was from American Radiolabeled Chemicals. Factor Xa protease was purchased from Roche Molecular Biochemicals. Precast Novex tris-glycine polyacrylamide gels and BenchMark ladder prestained molecular mass standards were obtained from Invitrogen. Hybond ECL nitrocellulose membranes and antirabbit IgG antibody conjugated to horseradish peroxidase were from Amersham Biosciences. The $\beta$-actin antibody (human) was from Cell Signaling, and Laemmli loading buffer was from Bio-Rad. The SuperSignal West Pico chemiluminescent substrate and CL-X Posure film were purchased from Pierce. All other reagents used were of the highest grade commercially available. $CuSO_4$ was mixed with 1,10-phenanthroline at a molar ratio of 1:3 (*36*). Throughout the text, the concentrations indicated for the $Cu^{II}$−(1,10-phenanthroline)$_3$ complex refer to molar copper concentrations.

*Site-Directed Mutagenesis.* Cys substitution mutagenesis was carried out using a pCD-based expression plasmid coding for a modified version of the rat $M_3$ muscarinic receptor referred to as M3′(3C)-Xa (ref *37*; Figure 1). This receptor construct contains a N-terminal hemagglutinin epitope tag and lacks all five potential N-terminal N-glycosylation sites. In addition, most endogenous Cys residues were substituted with either alanine or serine residues, except for C140, C220, and C532 (ref *37*; Figure 1). Importantly, the central portion of the i3 loop (A274−K469) was replaced by two factor Xa cleavage sites. For Cys substitution mutagenesis studies, we used the QuikChange site-directed mutagenesis kit (Stratagene), according to the instructions of the manufacturer. In the present study, we generated 20 M3′(3C)-Xa-based double Cys mutant $M_3$ receptors harboring one Cys substitution within the cytoplasmic end of TM V (L249−I253) and a second one within the cytoplasmic end of TM VI (A489−L492; Figure 1 and Table 1). The identity of all mutant receptors was confirmed by DNA sequencing.

*Cell Culture and Transient Expression of Cys-Substituted Mutant $M_3$ Muscarinic Receptors.* COS-7 cells were maintained in Dulbecco's modified Eagle's medium supplemented with 10% fetal bovine serum, 2 mM L-glutamine, 100 units/mL penicillin, and 100 $\mu$g/mL streptomycin at 37 °C in a humidified 5% $CO_2$ incubator. About 24 h prior to transfections, ~1 × $10^6$ cells were seeded into 100 mm dishes. Cells were transfected with 4 $\mu$g/dish of plasmid DNA coding for the M3′(3C)-Xa receptor or M3′(3C)-Xa-derived Cys-substituted mutant receptors. Transfections were carried out using the Lipofectamine Plus kit (Invitrogen), according to the instructions of the manufacturer. Transfected cells were incubated with 1 $\mu$M atropine for the last 24 h of culture, to increase receptor expression levels (*19, 20, 25–28*).

*Preparation of Membranes from Receptor-Expressing Cells.* COS-7 cells were harvested ~48 h after transfections. Initially, cells were washed twice (10 min each wash) with 10 mL of ice-cold phosphate-buffered saline (pH 7.4). This

washing step proved necessary for the complete removal of atropine, which was present in the culture medium during the last 24 h of culture. Subsequently, 2 mL of ice-cold buffer A (25 mM sodium phosphate and 5 mM $MgCl_2$ at pH 7.4) was added to each 100 mm dish, followed by a 15 min incubation at 4 °C. Cells were then scraped off the plates and homogenized using a Polytron tissue homogenizer (setting 5; 20 s). Cell homogenates were centrifuged for 15 min at 20000*g* at 4 °C. Membrane pellets were rehomogenized in 1 mL of ice-cold buffer A, frozen on dry ice, and stored at −70 °C until use. Protein concentrations were measured using the Micro BCA protein assay reagent kit (Pierce) with bovine serum albumin as a standard.

*Radioligand-Binding Studies.* Radioligand-binding assays were carried out using receptor-containing membrane preparations as described previously (*26*). In [$^3$H]NMS saturation binding studies, six concentrations of the radioligand ranging from 20 to 3000 pM were used. In carbachol competition binding assays, a fixed concentration of [$^3$H]NMS (500 pM) was used in the presence of 10 different concentrations of carbachol (concentration range from 5 nM to 10 mM). Binding reactions containing ~20 $\mu$g of membrane protein per tube were carried out at 22 °C for 2 h in a final volume of 1 mL of buffer A (see above). Reactions were terminated by rapid filtration over GF/C Brandel filters, followed by three washes (~4 mL per wash) with ice-cold distilled water. Nonspecific binding was determined in the presence of 1 $\mu$M atropine. Bound and free [$^3$H]-NMS were separated by rapid vacuum filtration, and radioactivity was quantified by liquid scintillation spectrometry. Binding data were analyzed using the nonlinear curve-fitting program Prism 4.0 (GraphPad).

*Receptor-Mediated Stimulation of Phosphatidylinositol (PI) Hydrolysis.* PI assays were carried out essentially as described previously (*26*). In brief, ~24 h after transfection in 100 mm dishes, COS-7 cells were trypsinized and seeded into six-well plates ($0.75 \times 10^6$ cells/well) and *myo*-[$^3$H]inositol (3 $\mu$Ci/mL) and atropine (1 $\mu$M) were added to the culture medium. On the next day (~24 later), cells were washed twice at room temperature (10 min each wash) with 2 mL of Hank's balanced salt solution to ensure the complete removal of atropine. Subsequently, cells were preincubated in 1 mL of the same salt solution containing 20 mM *N*-2-hydroxyethylpiperazine-*N*′-2-ethanesulfonic acid (HEPES) (pH 7.4) and 10 mM LiCl for 20 min at room temperature. Cells were then incubated with increasing concentrations of carbachol (final concentration from 1 nM to 1 mM) in the presence of 10 mM LiCl for 1 h at 37 °C. Reactions were terminated by replacing the assay buffer with 0.8 mL of 20 mM ice-cold formic acid, and the inositol monophosphate (IP) fraction was then isolated and quantitated as described previously (*26*). Carbachol $EC_{50}$ and $E_{max}$ values were derived from concentration–response curves using the nonlinear curve-fitting program Prism 4.0 (GraphPad).

*Oxidation, Solubilization, and Factor Xa Digestion of Double Cys Mutant $M_3$ Muscarinic Receptors.* Disulfide cross-linking studies were carried out essentially as described previously (*26*). In brief, receptor-containing membranes prepared from one 100 mm dish of transfected COS-7 cells (~1 mg of protein) were suspended in 1 mL of buffer A containing 25 $\mu$M $Cu^{II}$−phenanthroline, either in the presence or absence of different muscarinic ligands. Oxidation reactions were carried out for 10 min at room temperature (22 °C), followed by the addition of ethylenediaminetetraacetic acid (EDTA) and *N*-ethylmaleimide (10 mM each) and a 10 min incubation on ice. Membrane proteins were then solubilized by incubating samples with 1.2% digitonin for 2 h at 4 °C, as described in detail by Han et al. (*26*). Receptor-containing membrane lysates (~15 $\mu$g of protein) were then treated in 30 $\mu$L of factor Xa digestion buffer with factor Xa protease (final concentration of 0.1 $\mu$g/$\mu$L) at room temperature for 16 h. Reactions were terminated by the addition of 1 $\mu$L of mammalian protease inhibitor mixture (1:25 dilution; *26*). Samples were then used either directly for sodium dodecyl sulfate−polyacrylamide gel electrophoresis (SDS−PAGE) or stored at −70 °C until needed.

*Western-Blotting Studies.* SDS−PAGE, Western-blotting, and enhanced chemiluminescence (ECL) detection of receptor proteins were performed as described in detail previously (*28*). In brief, receptor-containing membrane lysates that had been treated with factor Xa were incubated with Laemmli loading buffer for 30 min at 37 °C, under either nonreducing or reducing conditions [in the absence or presence of 50 mM dithiothreitol (DTT), respectively]. Samples were then loaded onto 10–20% Tris-glycine polyacrylamide gels and run at 125 V in the presence of 0.1% SDS. Western-blotting studies were carried out as described (*28*), using a rabbit polyclonal anti-$M_3$ receptor antibody directed against the C-terminal 18 amino acids of the rat $M_3$ receptor sequence (*38*). $M_3$ receptor proteins were visualized by the use of ECL reagents and autoradiography. The intensities of immunoreactive bands were quantitated by scanning densitometry using the program NIH ImageJ (NIH).

## RESULTS

*Generation of Double Cys Mutant $M_3$ Muscarinic Receptors.* To gain insight into the conformational changes associated with muscarinic receptor activation, we subjected a series of double Cys mutant $M_3$ muscarinic receptors to an *in situ* disulfide cross-linking approach (*19, 20, 25–28*). All Cys substitutions were introduced into a modified version of the $M_3$ muscarinic receptor lacking most native Cys residues and containing a pair of factor Xa cleavage sites within the i3 loop (referred to as "M3′(3C)-Xa" receptor throughout the paper; Figure 1). We demonstrated previously that the M3′(3C)-Xa background receptor retains the ability to bind muscarinic ligands with high affinity and to productively couple to G proteins (*37*). Specifically, we generated 20 double Cys mutant $M_3$ receptors harboring one Cys substitution within the cytoplasmic end of TM V (L249−I253) and a second one within the cytoplasmic end of TM VI (A489−L492; Figure 1 and Table 1). These receptors were transiently expressed in COS-7 cells and subsequently characterized in pharmacological and biochemical studies.

*Ligand-Binding Properties of Double Cys Mutant $M_3$ Muscarinic Receptors.* To increase the expression levels of the double Cys mutant $M_3$ muscarinic receptors and thereby facilitate their detection via Western blotting, transfected COS-7 cells were incubated with atropine (1 $\mu$M) for the last 24 h of culture (*19, 20, 25–28*). The ligand-binding properties of all mutant receptors were characterized in radioligand-binding studies, using [$^3$H]-NMS, a classical muscarinic antagonist, as a radioligand. [$^3$H]-NMS saturation

binding studies with receptor-containing membrane preparations demonstrated that all double Cys mutant $M_3$ receptors were expressed at levels ($B_{max}$) > 1.8 pmol/mg of membrane protein (Table 1). All receptors were able to bind [$^3$H]-NMS with high affinity (range of [$^3$H]-NMS $K_D$ values of 102–264 pM; Table 1). Moreover, [$^3$H]-NMS/carbachol inhibition binding experiments showed that all double Cys mutant receptors bound carbachol, a muscarinic agonist, with affinities that were similar to or even higher than that observed with the M3′(3C)-Xa construct (range of carbachol $K_i$ values of ~1–59 $\mu$M; Table 1). Specifically, we noted that all constructs containing the Y250C and L492C point mutations consistently showed considerably higher carbachol affinities (3–22-fold) than the M3′(3C)-Xa construct, from which all Cys mutant $M_3$ receptors were derived. This observation is consistent with the concept that the molecular properties of the orthosteric binding site for muscarinic agonists can be affected allosterically by structural modification of the intracellular receptor surface (*23, 39*).

*Functional Activity of Double Cys Mutant $M_3$ Muscarinic Receptors.* To determine the ability of the different mutant receptors to couple to heterotrimeric G proteins, we studied carbachol-dependent changes in IP accumulation. Carbachol stimulation led to a significant increase in IP accumulation in all mutant receptors studied (Table 1), indicating that all investigated double Cys mutant receptors retained functional activity. Notably, all mutant receptors containing the Q490C point mutation showed significant elevations in basal IP levels (~2–7-fold as compared to the M3′(3C)-Xa construct; Table 1). Moreover, these constructs also displayed significant increases in carbachol potencies (~6–13-fold as compared to the M3′(3C)-Xa construct; Table 1). These observations are consistent with previous findings that the Q490L point mutation renders the $M_3$ muscarinic receptor constitutively active (*40*). In contrast, most of the remaining double Cys receptors showed reduced basal signaling, as compared to the M3′(3C)-Xa receptor (Table 1). It is likely that the various point mutations, which were introduced into receptor regions known to be critically involved in receptor/G protein interactions (*6*), reduced basal receptor activity by decreasing the probability that the mutant receptors spontaneously adopted the active receptor conformation. In addition, reduced receptor expression levels ($B_{max}$) may also contribute to the observed reduction in basal signaling, at least in the case of some of the mutant receptors (Table 1). The low basal activity of most investigated mutant receptors also offers a likely explanation for the observation that many double Cys receptors showed $E_{max}$ values (expressed as fold stimulation in IP accumulation above basal IP levels) that were significantly greater than the control value ($E_{max}$ of the M3′(3C)-Xa construct; Table 1). These receptors include L249C/A489C, L249C/T491C, Y250C/A489C, Y250C/L492C, R252C/A489C, R252C/T491C, I253C/A489C, and I253C/T491C. Most double Cys mutant receptors, except for those containing the Q490L point mutation and the L249C/L492C, W251C/L492C, and R252C/L492C constructs, also showed significant reductions in carbachol potencies (~2–70-fold as compared to the M3′(3C)-Xa construct; Table 1). These decreases in carbachol potencies are most likely due to mutation-induced impairments in the efficiency of receptor/G protein coupling and/or reduced receptor densities ($B_{max}$).

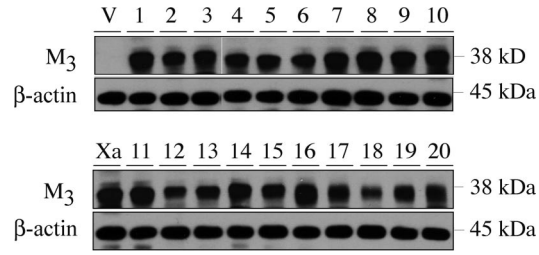


FIGURE 2: Detection of double Cys mutant $M_3$ receptors via Western blotting. Membranes were prepared from COS-7 cells transfected with the following mutant $M_3$ receptor constructs (or vector DNA). Upper panel: V (vector), 1 (L249C/A489C), 2 (Y250C/A489C), 3 (W251C/A489C), 4 (R252C/A489C), 5 (I253C/A489C), 6 (L249C/Q490C), 7 (Y250C/Q490C), 8 (W251C/Q490C), 9 (R252C/Q490C), and 10 (I253C/Q490C). Lower panel: Xa (M3′(3C)-Xa), 11 (L249C/T491C), 12 (Y250C/T491C), 13 (W251C/T491C), 14 (R252C/T491C), 15 (I253C/T491C), 16 (L249C/L492C), 17 (Y250C/L492C), 18 (W251C/L492C), 19 (R252C/L492C), and 20 (I253C/L492C). Membranes prepared from transfected COS-7 cells were processed for Western-blotting studies (nonreducing conditions) as described in the caption of Figure 4 (for more details, see the Experimental Procedures), except that the factor Xa incubation step was omitted. Equal amounts of protein (5 $\mu$g) were loaded in each lane. The ~38 kDa full-length receptor bands detected by the anti-M3 antibody are shown. For control purposes, all blots were also reprobed with an anti-$\beta$-actin antibody.

*Disulfide Cross-Linking Studies.* Consistent with the results of the [$^3$H]-NMS saturation binding studies, Western-blotting studies using a polyclonal antibody directed against the C-terminal portion of the rat $M_3$ muscarinic receptor (referred to as "anti-$M_3$ antibody") showed that all newly generated double Cys mutant receptors could be easily detected in membrane lysates prepared from transfected COS-7 cells (Figure 2).

To explore the potential proximity of the Cys pairs present in the 20 double Cys mutant receptors, we examined their ability to form intramolecular disulfide bonds. The general strategy used to detect the formation of intramolecular disulfide bonds in these mutant receptors is summarized in Figure 3. For disulfide cross-linking studies, we used receptor-containing membranes prepared from transfected COS-7 cells. To promote the formation of disulfide bonds, membrane samples were incubated with a low concentration of the mild oxidizing agent, $Cu^{II}$−phenanthroline (Cu−Phen, 25 $\mu$M; 10 min of incubation at room temperature), either in the absence or presence of muscarinic ligands. Subsequently, receptors were solubilized, digested to completion with factor Xa, and subjected to SDS−PAGE and Western blotting (nonreducing conditions). Under these conditions, the appearance of a full-length receptor band (~38 kDa) is indicative of successful disulfide cross-linking (*19, 25*). Previous studies indicated that this ~38 kDa immunoreactive species corresponds to properly folded cell-surface receptors (*19, 25*).

In an initial set of studies, we examined whether incubation of samples with the muscarinic agonist, carbachol (1 mM), led to activity-dependent changes in disulfide cross-linking patterns. The results of these studies are summarized in Figure 4. Most of the analyzed double Cys mutant receptors failed to yield a detectable cross-linking signal, either in the absence or presence of carbachol. Strikingly, carbachol treatment promoted the formation of disulfide bonds in six of the studied mutant receptors (Y250C/T491C, Y250C/L492C, I253C/A489C, I253C/Q490C, I253C/T491C, and

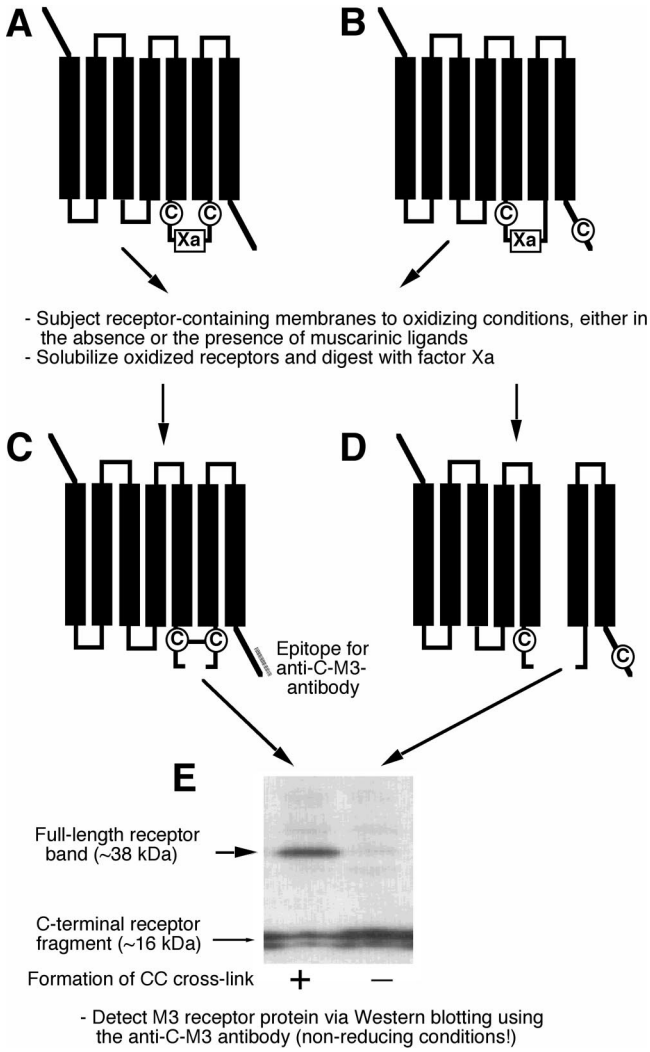


FIGURE 3: Scheme outlining the strategy used to detect the formation of intramolecular disulfide bonds in double Cys mutant $M_3$ muscarinic receptors. Pairs of Cys residues were introduced into the M3′(3C)-Xa background receptor (see Figure 1), one Cys N-terminal and the other one C-terminal of the factor Xa cleavage site. When two Cys residues lie adjacent to each other in the 3D structure of the receptor, they have the potential to form a disulfide bridge (A and C). Upon cleavage with factor Xa, the disulfide bridge will keep the two cleavage products covalently linked (A and C). As a result, a full-length receptor band (~38 kDa in size) will appear on Western blots run under nonreducing conditions (left lane in E). In contrast, when the two introduced Cys residues are not close to each other in the 3D structure of the receptor, they are unable to form a disulfide bridge (B and D). As a consequence, factor Xa digestion will yield two separate cleavage products and a full-length receptor band will not appear on Western blots run under nonreducing conditions (right lane in E).

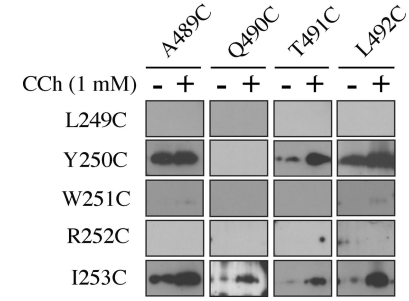


FIGURE 4: Carbachol promotes the formation of disulfide bonds in several double Cys mutant $M_3$ muscarinic receptors. Membranes were prepared from COS-7 cells expressing the indicated double Cys mutant $M_3$ muscarinic receptors. Receptors were oxidized with Cu−Phen (25 $\mu$M) in the absence or presence of the muscarinic agonist, carbachol (CCh, 1 mM), digested with factor Xa, and subjected to Western-blotting analysis (nonreducing conditions), using the anti-M3 antibody (for details, see the Experimental Procedures). The bands shown correspond to the ~38 kDa full-length receptor species, which is indicative of successful disulfide cross-linking (*19, 25*). Note that CCh promoted disulfide cross-link formation in six of the investigated double Cys mutant receptors (Y250C/T491C, Y250C/L492C, I253C/A489C, I253C/Q490C, I253C/T491C, and I253C/L492C). Another mutant receptor, Y250C/A489C, gave a cross-linking signal that was similar in intensity in the absence or presence of CCh. All Western blots shown are representative of three independent experiments. In each individual experiment, identical amounts of protein were loaded in each lane (~5 $\mu$g/lane).

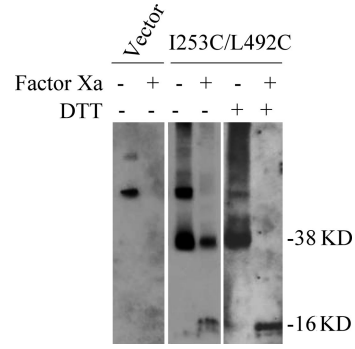


FIGURE 5: Example Western blots for one of the analyzed mutant receptors (I253C/L492C) showing entire blots. Samples were oxidized in the presence of 1 mM carbachol as indicated in the caption of Figure 4. Whereas one set of samples was treated with factor Xa, a duplicate set of samples was not treated with the protease. Samples were then run under nonreducing or reducing conditions in the absence or presence of DTT (50 mM), respectively. The anti-M3 antibody was used to detect $M_3$ receptor-specific bands. Note that DTT treatment of factor Xa-digested samples leads to the disappearance of the ~38 kDa receptor species and the appearance of a ~16 kDa immunoreactive species (corresponding to the receptor region C-terminal of the Xa cleavage site), indicative of disulfide bond formation (*19, 25*).

I253C/L492C; Figure 4), indicative of carbachol-induced changes in receptor conformation. One of the mutant receptors, Y250C/A489C, yielded a prominent cross-linking signal, which remained unchanged in intensity after carbachol treatment (Figure 4). Full-length receptor bands (~38 kDa) were not observed when Western-blotting studies were carried out under reducing conditions (data not shown), indicating that they were not caused by incomplete digestion by factor Xa.

Figure 5 provides example Western blots for one of the mutant receptors (I253C/L492C) showing entire blots. Samples were oxidized in the presence of 1 mM carbachol (see above) and then either digested with factor Xa or not treated with the protease. Receptor-containing samples were then run under nonreducing or reducing conditions in the absence or presence of DTT (50 mM), respectively.

To determine percent cross-linking efficiencies (the percentage of total receptor population that underwent disulfide cross-linking), rather than simply changes in disulfide cross-linking relative to the unoccupied receptor, the carbachol-sensitive double Cys mutant receptors were first oxidized in the presence of carbachol (1 mM) as described above. Solubilized receptors were then divided into two equal aliquots and either digested with factor Xa or left untreated. Receptor-containing samples were then subjected to Western-

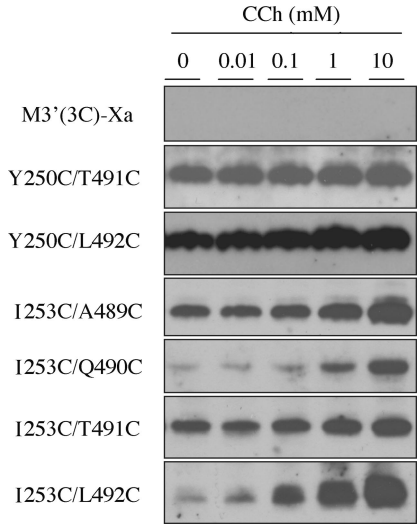


FIGURE 6: Carbachol increases disulfide cross-link formation in six of the analyzed double Cys mutant $M_3$ muscarinic receptors in a concentration-dependent fashion. Membranes were prepared from COS-7 cells expressing the indicated double Cys mutant receptors. Receptors were oxidized with Cu−Phen (25 $\mu$M) in the presence of increasing concentrations of carbachol (CCh), digested with factor Xa, and subjected to Western-blotting analysis (nonreducing conditions), using the anti-M3 antibody (for details, see the Experimental Procedures). The ~38 kDa full-length receptor bands, which are indicative of successful disulfide cross-linking (*19, 25*), are shown. The data shown are representative of three independent experiments. In each individual experiment, identical amounts of protein were loaded in each lane (~5 $\mu$g/lane).

blotting analysis under nonreducing conditions, and the intensities of the immunoreactive 38 kDa bands were quantitated by scanning densitometry. To determine percent cross-linking efficiencies, the intensities of the 38 kDa bands observed following factor Xa digestion (corresponding to cross-linked receptors) were divided by the intensities of the 38 kDa bands in control samples that had not been treated with factor Xa (corresponding to total receptors). Using this approach, the following cross-linking efficiencies were observed [means ± standard error of the mean (SEM) of three to five independent experiments]: Y250C/T491C (20 ± 3%), Y250C/L492C (37 ± 1%), I253C/A489C (36 ± 2%), I253C/Q490C (8 ± 1%), I253C/T491C (21 ± 5%), and I253C/L492C (42 ± 8%).

*Intensity of Disulfide Cross-Linking Signals Increases with Increasing Carbachol Concentrations.* To further examine the agonist dependence of the disulfide cross-linking signals displayed by the Y250C/T491C, Y250C/L492C, I253C/A489C, I253C/Q490C, I253C/T491C, and I253C/L492C receptors (see Figure 4), we carried out additional cross-linking experiments in which these six receptors were oxidized in the presence of increasing carbachol concentrations (0.01–10 mM). In all six double Cys mutant receptors, carbachol induced concentration-dependent increases in the intensity of the 38 kDa cross-linking signal (nonreducing conditions; Figure 6). A summary of carbachol $EC_{50}$ and $E_{max}$ values is given in Table 2.

*Disulfide Bonds Form Intramolecularly.* As has been shown for a large number of GPCRs (*41, 42*), $M_3$ muscarinic receptors are known to form dimers or oligomers (*43, 44*). To rule out the possibility that the carbachol-induced formation of disulfide bonds observed with the Y250C/T491C, Y250C/L492C, I253C/A489C, I253C/Q490C, I253C/T491C, and I253C/L492C receptors was due to the formation of intermolecular disulfide bridges (involving Cys residues located on different receptor molecules), we carried out an additional set of studies. We first generated six M3′(3C)-Xa-based mutant receptors containing the Y250C, I253C, A489C, Q490C, T491C, and L492C single Cys substitutions. All six mutant receptors could be easily detected in Western-blotting studies using membranes prepared from transfected COS cells that had not been treated with factor Xa (Figure 7A). After treatment of oxidized samples (25 $\mu$M Cu−Phen) with factor Xa, full-length receptor bands could no longer be observed, either in the absence or presence of carbachol, consistent with the concept that disulfide bonds are unable to form in the single Cys mutant receptors (Figure 7A).

We then cotransfected COS-7 cells with the following pairs of single Cys mutant receptor constructs: Y250C + T491C, Y250C + L492C, I253C + A489C, I253C + Q490C, I253C + T491C, and I253C + L492C. After oxidation of membrane homogenates with Cu−Phen (25 $\mu$M) and factor Xa treatment, no disulfide cross-linking signals (38 kDa bands) were detectable in these coexpression studies (Figure 7B), as observed with the single Cys mutant receptors. These data, together with the results shown in Figures 4 and 6, strongly support the concept that the Cys residues contained in the Y250C/T491C, Y250C/L492C, I253C/A489C, I253C/Q490C, I253C/T491C, and I253C/L492C double Cys mutant receptors formed intramolecular rather than intermolecular disulfide bridges.

*Effect of Inverse Muscarinic Agonists on Disulfide Bond Formation in Double Cys Mutant $M_3$ Receptors.* To examine the effects of different muscarinic ligands on $M_3$ muscarinic receptor structure, we carried out additional cross-linking studies with the Y250C/T491C, Y250C/L492C, I253C/A489C, I253C/Q490C, I253C/T491C, and I253C/L492C receptors. In a fashion similar to carbachol (1 mM), the physiological muscarinic agonist, acetylcholine (1 mM), promoted the formation of disulfide cross-links in all six double Cys mutant receptors (Figure 8). A completely different pattern was observed when samples were oxidized in the presence of atropine or NMS. Traditionally, atropine and NMS have been considered conventional muscarinic antagonists. Recently, however, these agents have been reclassified as inverse muscarinic agonists, because of their ability to suppress signaling by constitutively active mutant muscarinic receptors (*45, 46*). While muscarinic agonists facilitated the formation of disulfide bonds in the I253C/A489C, I253C/T491C, and I253C/L492C double Cys mutant receptors, treatment with the inverse agonists atropine and NMS (1 $\mu$M each) impaired basal disulfide cross-linking exhibited by these three receptors (Figure 8). Interestingly, treatment with atropine or NMS of membrane samples containing the Y250C/T491C or Y250C/L492C receptors led to enhanced disulfide cross-linking, similar to the effects exerted by muscarinic agonists (Figure 8) [percent increase in cross-linking above basal (=100%). Y250C/T491C receptor: carbachol, 131 ± 8; acetylcholine, 175 ± 8; atropine, 157 ± 10; and NMS, 149 ± 15. Y250C/L492C receptor: carbachol, 134 ± 10; acetylcholine, 134 ± 11; atropine, 125 ± 6; and NMS, 150 ± 8].

Those double Cys mutant receptors that did not display any agonist-dependent changes in disulfide cross-linking also failed to exhibit significant changes in disulfide cross-linking

Table 2: Quantification of the Effects of Carbachol (Agonist) and NMS (Inverse Agonist) on Disulfide Bond Formation in Double Cys Mutant $M_3$ Muscarinic Receptors[a]

| | carbachol | | NMS | |
|---|---|---|---|---|
| receptor | $E_{max}$[b] (% of control) (=100%) | $EC_{50}$[c] ($\mu$M) | $E_{max}$ (% of control) (=100%) | $EC_{50}/IC_{50}$[d] (pM) |
| Y250C/T491C | 149 ± 16 | 780 ± 280 | 153 ± 1 | 170 ± 50 |
| Y250C/L492C | 147 ± 13 | 84 ± 24 | 152 ± 18 | 270 ± 100 |
| I253C/A489C | 159 ± 30 | 654 ± 94 | 41 ± 14 | 40 ± 9 |
| I253C/Q490C | 336 ± 89 | 806 ± 47 | ND[e] | ND |
| I253C/T491C | 142 ± 1 | 171 ± 54 | 60 ± 13 | 20 ± 4 |
| I253C/L492C | 783 ± 366 | 93 ± 42 | 20 ± 6 | 540 ± 40 |

[a] Membranes were prepared from COS-7 cells expressing the indicated double Cys mutant $M_3$ receptors and processed for disulfide cross-linking and Western-blotting studies (nonreducing conditions), as described under the Experimental Procedures. Disulfide cross-linking studies were carried out in either the absence of ligands (control) or presence of increasing concentrations of the full muscarinic agonist, carbachol, or the inverse muscarinic agonist, NMS. The intensities of immunoreactive bands corresponding to cross-linked receptors were determined by scanning densitometry (NIH ImageJ). In each individual experiment, the extent of disulfide cross-linking observed in the absence of ligands was set equal to 100%. Data are given as means ± SEM of three independent experiments. [b] Maximum degree of disulfide cross-linking compared to cross-linking in the absence of ligands (control; 100%). [c] Carbachol concentration at which the inhibition of disulfide cross-linking corresponds to half of the $E_{max}$. [d] NMS concentration at which the stimulation ($EC_{50}$) or inhibition ($IC_{50}$) of disulfide cross-linking corresponds to half of the $E_{max}$. [e] ND = lack of disulfide cross-linking at the highest NMS concentration used (10 nM).

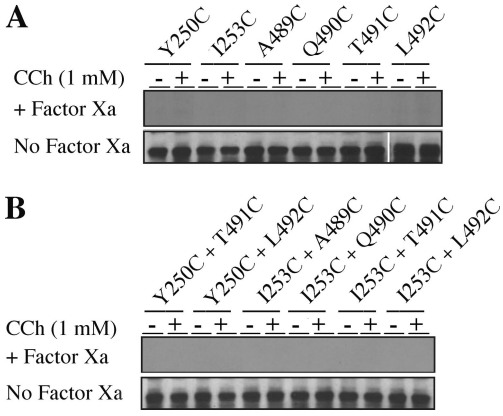


FIGURE 7: Carbachol-induced disulfide cross-linking observed with six of the analyzed double Cys mutant $M_3$ muscarinic receptors does not involve intermolecular disulfide bonds. In A, COS-7 cells were transfected with the following M3′(3C)-Xa-based single Cys receptor constructs: Y250C, I253C, A489C, Q490C, T491C, and L492C. In B, COS-7 cells were cotransfected with the following pairs of single Cys mutant receptors: Y250C + T491C, Y250C + L492C, I253C + A489C, I253C + Q490C, I253C + T491C, and I253C + L492C. Receptor-containing membrane preparations were first oxidized with Cu−Phen (25 $\mu$M), either in the absence or presence of the muscarinic agonist, carbachol (CCh, 1 mM). Samples were then treated with factor Xa (top rows in A and B) and subjected to Western-blotting analysis (nonreducing conditions), using the anti-M3 antibody. In parallel, a second set of samples was processed in the same fashion, except that the factor Xa digestion step was omitted (lower rows in A and B), to ensure that all receptors were detectable via Western blotting. All bands shown correspond to the ~38 kDa full-length receptor species. The absence of 38 kDa bands in factor Xa-treated samples in B indicates that disulfide bonds do not form intermolecularly. Representative blots are shown. Two additional experiments gave similar results. In each individual experiment, identical amounts of protein were loaded in each lane (~5 $\mu$g/lane).

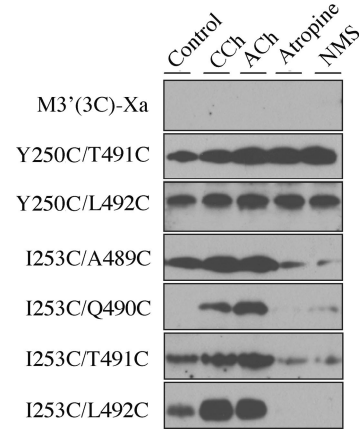


FIGURE 8: Effects of full versus inverse muscarinic agonists on disulfide cross-link formation in six of the analyzed double Cys mutant $M_3$ muscarinic receptors. Membranes were prepared from COS-7 cells expressing the indicated mutant receptors and processed for disulfide cross-linking studies as described under the Experimental Procedures. Samples were oxidized with Cu−Phen (25 $\mu$M) in the absence of ligands (control), the presence of CCh (full agonist; 1 mM), acetylcholine (ACh, full agonist; 1 mM), atropine (inverse agonist; 1 $\mu$M), or NMS (inverse agonist; 1 $\mu$M). Receptors were then digested with factor Xa and subjected to Western-blotting analysis (nonreducing conditions), using the anti-M3 antibody (for details, see the Experimental Procedures). Whereas the two full agonists (CCh and ACh) facilitated the formation of disulfide bonds in all six analyzed double Cys mutant receptors, incubation with the two inverse muscarinic agonists (atropine and NMS) led to reduced disulfide cross-linking in three of the receptors (I253C/A489C, I253C/T491C, and I253C/L492C). Interestingly, the two inverse agonists, similar to the two full agonists, facilitated disulfide bond formation in the Y250C/T491C and Y250C/L492C receptors. The immunoreactive bands shown correspond to the ~38 kDa full-length receptor species, which are observed following successful disulfide cross-linking (*19, 25*). Representative blots are shown. Two additional experiments gave similar results. In each individual experiment, identical amounts of protein were loaded in each lane (~5 $\mu$g/lane).

patterns in the presence of the inverse muscarinic agonist, atropine (10 nM; data not shown).

*Inverse Muscarinic Agonist, NMS, Modulates the Intensity of Disulfide Cross-Linking Signals in a Concentration-Dependent Fashion.* We carried out additional cross-linking experiments in which the Y250C/T491C, Y250C/L492C, I253C/A489C, I253C/Q490C, I253C/T491C, and I253C/L492C receptors were oxidized in the presence of increasing concentrations (0.01–10 nM) of the inverse muscarinic agonist, NMS. In all cases, NMS treatment led to concentration-dependent changes in the intensity of the 38 kDa cross-linking signal (nonreducing conditions; Figure 9). A summary of NMS $EC_{50}/IC_{50}$ and $E_{max}$ values is given in Table 2.

*Effect of Atropine and NMS on Basal Signaling by Double Cys Mutant $M_3$ Receptors in PI Assays.* To study the effects of atropine and NMS on basal signaling by the Y250C/T491C, Y250C/L492C, I253C/A489C, I253C/Q490C, I253C/

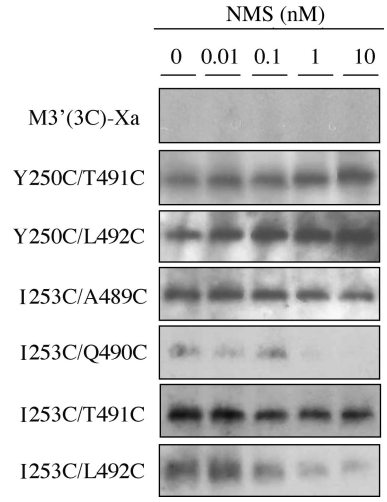


FIGURE 9: NMS modulates disulfide cross-link formation in six of the analyzed double Cys mutant $M_3$ muscarinic receptors in a concentration-dependent fashion. Membranes were prepared from COS-7 cells expressing the indicated double Cys mutant receptors. Receptors were oxidized with Cu−Phen (25 $\mu$M) in the presence of increasing concentrations of the inverse muscarinic agonist, NMS, digested with factor Xa, and subjected to Western-blotting analysis (nonreducing conditions), using the anti-M3 antibody (for details, see the Experimental Procedures). The ~38 kDa full-length receptor bands, which are indicative of successful disulfide cross-linking (*19, 25*), are shown. The data shown are representative of three independent experiments. In each individual experiment, identical amounts of protein were loaded in each lane (~5 $\mu$g/lane).

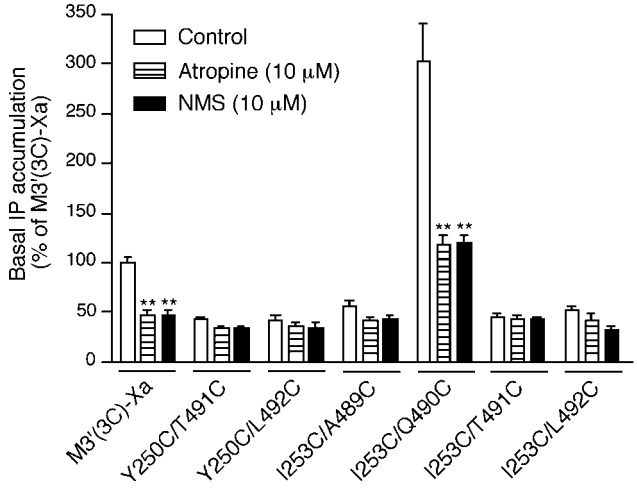


FIGURE 10: Effect of atropine and NMS on basal signaling by selected double Cys mutant $M_3$ muscarinic receptors. COS-7 cells expressing the indicated receptor constructs were incubated in 12-well plates at 37 °C for 1 h in the absence or presence of atropine or NMS (10 $\mu$M each). IP accumulation was measured as described under the Experimental Procedures. Data are presented as means ± SE and are representative of three independent experiments. (**) $p < 0.01$, as compared to IP levels measured in the absence of ligands (Student's *t* test).

T491C, and I253C/L492C double Cys mutant receptors, we carried out a series of functional studies (PI assays). Both ligands significantly suppressed basal IP accumulation in cells transfected with the M3′(3C)-Xa receptor from which all double Cys mutant receptors were derived (Figure 10). Similarly, both atropine and NMS greatly reduced the increase in basal signaling displayed by the constitutively active I253C/Q490C mutant receptor (Figure 10). These findings are consistent with the notion that atropine and NMS act as inverse muscarinic agonists. In five of the six analyzed double Cys mutant receptors (Y250C/T491C, Y250C/L492C, I253C/A489C, I253C/T491C, and I253C/L492C), atropine and NMS did not lead to significant reductions in basal IP accumulation (Figure 10). However, in most cases, atropine- or NMS-treated samples showed a trend toward lower basal IP levels. One possible explanation for this observation is that the Y250C/T491C, Y250C/L492C, I253C/A489C, I253C/T491C, and I253C/L492C receptors showed significantly reduced basal signaling (as compared to the M3′(3C)-Xa construct from which they were derived; Table 1 and Figure 10), making it difficult to reveal the inverse agonist activity of atropine and NMS at these receptors.

## DISCUSSION

A vast number of studies has shown that multiple receptor domains are involved in productive receptor/G protein coupling (*1, 2, 4, 6*). For example, several lines of evidence suggest that the cytoplasmic ends of TM V and VI of class I GPCRs contain key residues critical for G protein recognition and activation (*1, 2, 4, 6*). On the other hand, amino acids located within the top portions of TM V and VI are known to be important for ligand binding to many class I GPCRs, including GPCRs for biogenic amines, such as the adrenergic and muscarinic receptors (*1, 2, 4, 6*). A likely scenario therefore is that agonist-mediated receptor activation involves a conformational rearrangement of the cytoplasmic ends of TM V and VI, which is required for productive receptor/G protein interactions.

Consistent with this concept, biochemical and biophysical studies carried out with the photoreceptor, rhodopsin, suggest a reorientation of the cytoplasmic end of TM VI and changes in the relative disposition of TM VI and III (*7, 8*). Similar results have been obtained with class I GPCRs that are activated by small diffusible ligands, including the $\beta_2$-adrenergic receptor (*14–18*) and the $M_3$ muscarinic receptor (*19, 20*).

In contrast, it remains unclear at present whether agonist-mediated activation of class I GPCRs also leads to major conformational changes of the cytoplasmic end of TM V. To address this question, we used the $M_3$ muscarinic receptor, a prototypic class I biogenic amine GPCR, as a model system. Specifically, we employed an *in situ* disulfide cross-linking strategy (*19, 20, 25–28*) that is carried out with Cys-substituted mutant $M_3$ receptors present in their native membrane environment. In the present study, we analyzed a series of double Cys mutant $M_3$ muscarinic receptors, all of which contained a Cys residue at the bottom of TM V ((L249−I253) and a second Cys residue within the cytoplasmic end of TM VI (A489−L492; Figure 1 and Table 1). Structural evidence indicates that the cytoplasmic ends of TM V and VI are located adjacent to each other in the 3D structure of class I GPCRs (*12, 13*). We therefore reasoned that the introduced TM VI Cys residues might function as potential reporter residues to detect ligand-induced conformational changes involving the cytoplasmic segment of TM V.

In a previous disulfide cross-linking study (*19*), we determined the ability of a Cys residue introduced at the TM V/i3 loop boundary (Y254C; Figure 1) to form activity-dependent disulfide bonds with Cys residues introduced into the cytoplasmic segment of TM VI (K484−S493). We found

that agonist treatment promoted the formation of disulfide cross-links in 4 of the 10 analyzed mutant receptors (Y254C/A489, Y254C/Q490C, Y254C/T491C, and Y254C/L492C). Because A489, Q490, T491, and L492 are predicted to be located within an α-helical domain (TM VI), this cross-linking pattern suggested that $M_3$ receptor activation is associated with a pronounced conformational change (e.g., a rotational movement) of the cytoplasmic end of TM VI (*19*). The cross-linking study by Ward et al. (*19*) also indicated that agonist binding to the $M_3$ receptor increases the proximity between the cytoplasmic ends of TM V and VI. A similar movement has been proposed for the $\beta_2$-adrenergic receptor based on fluorescence spectroscopic studies (*30*). In these studies (*19, 30*), only a single TM V residue was used as a reporter to detect activity-dependent changes in the structure of TM VI. Thus, these studies were not designed to reveal potential conformational changes involving the cytoplasmic portion of TM V. In the present study, we therefore generated a series of double Cys mutant $M_3$ receptors, in which five consecutive TM V residues (L249−I253) were subjected to Cys substitution mutagenesis.

Radioligand-binding studies showed that all double Cys mutant receptors were able to bind the muscarinic antagonist/inverse agonist (see below), [$^3$H]NMS, and the muscarinic agonist, carbachol, with high affinities. In addition, PI assays demonstrated that all mutant receptors retained the ability to activate G proteins, suggesting that all mutant receptor proteins were folded properly. However, in the PI assays, many double Cys mutant receptors showed significant reductions in carbachol potency and basal activity, as compared to the M3′(3C)-Xa construct (Table 1). This finding was not unexpected because the targeted muscarinic receptor regions are known to play important roles in determining the efficiency of receptor/G protein interactions (*21–23*).

Disulfide cross-linking studies demonstrated that carbachol and acetylcholine, two full muscarinic agonists, promoted the formation of disulfide bonds in 6 of the 20 analyzed double Cys mutant $M_3$ receptors (Y250C/T491C, Y250C/L492C, I253C/A489C, I253C/Q490C, I253C/T491C, and I253C/L492C). This observation suggests that $M_3$ receptor activation leads to conformational changes that increase the proximity between the cytoplasmic ends of TM V and VI, consistent with the outcome of a previous cross-linking study (*19*). Control experiments demonstrated that the various disulfide bonds formed intramolecularly rather than between different receptor molecules.

We recently established a 3D model of the rat $M_3$ muscarinic receptor using homology modeling based on the high-resolution X-ray structure of the inactive state of bovine rhodopsin (*26*). The $M_3$ receptor model (Figure 11) shows that Y250 and I253 (both located in TM V) are located in close proximity to A489 and L492 (both located in TM VI) in the inactive state of the receptor (estimated distances between the Cα atoms of Y250/I253 and A489/L492 of ~9–11 Å). In contrast to A489 and L492, the two remaining TM VI residues targeted in the present study, Q490 and T491, do not project to TM V in the inactive state of the receptor (Figure 11) (Q490 and T491 are predicted to face the lipid bilayer and TM VII, respectively). The observation that muscarinic agonists do not only promote the formation of disulfide bonds in the Y250C/L492C, I253C/A489C, I253C/T491C, and I253C/L492C constructs but also in the Y250C/T491C and I253C/Q490C receptors therefore indicates that $M_3$ receptor activation involves a major structural rearrangement of the cytoplasmic end of TM VI (*19*). As discussed in detail previously (*19*), these findings are consistent with an activity-dependent rotational movement of the cytoplasmic end of TM VI and/or a partial unraveling of this helical domain.

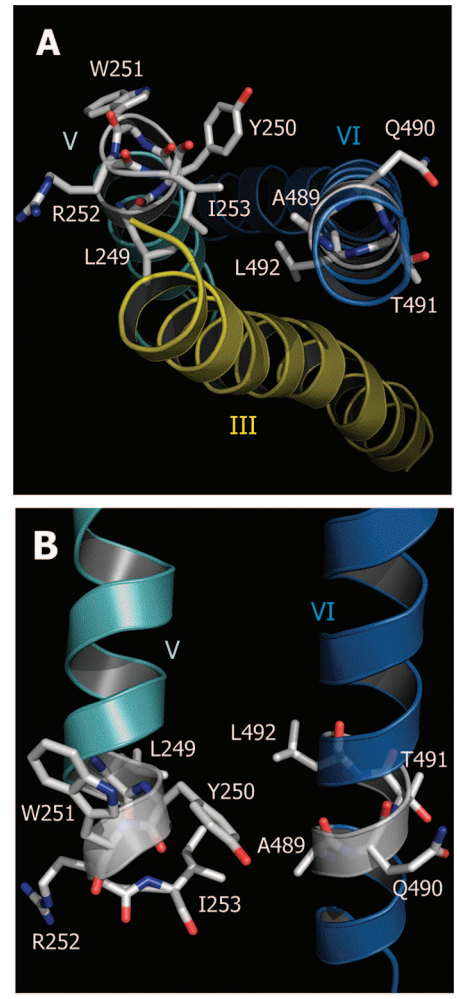


FIGURE 11: Predicted location of $M_3$ muscarinic receptor residues targeted in the present study. A 3D model of the inactive state of the rat $M_3$ muscarinic receptor was built via homology modeling using the high-resolution X-ray structure of bovine rhodopsin as a template (*12, 26*). (A) Cytoplasmic view of a selected region of the intracellular surface of the $M_3$ receptor. (B) Side view of the $M_3$ receptor, showing the cytoplasmic portions of TM V and VI. The side chains of the TM V and VI residues that were subjected to Cys substitution mutagenesis are highlighted. Among the five TM V residues that were replaced by Cys residues, only Y250 and I253 are predicted to face TM VI. Amino acid position numbers according to the Ballesteros/Weinstein GPCR nomenclature (*51*) are L249$^{5.57}$, Y250$^{5.58}$, W251$^{5.59}$, R252$^{5.60}$, I253$^{5.61}$, A489$^{6.34}$, Q490$^{6.35}$, T491$^{6.36}$, and L492$^{6.37}$.

It should be noted in this context that the carbachol-mediated changes in disulfide cross-linking patterns observed with six of the investigated double Cys mutant receptors can occur at different time points during receptor activation (through a process referred to as "disulfide trapping"; ref (*7*)). Clearly, the observed agonist-dependent increases in disulfide bond formation do not reflect a single receptor conformation corresponding to the activated state of the receptor.

Interestingly, muscarinic agonists failed to induce the formation of disulfide bonds in all double Cys mutant $M_3$ receptors containing the L249C, W251C, or R252C TM V substitutions. In contrast to Y250 and I253 (see above), L249, W251, and R252 do not face TM VI but project to the bottom of TM III (L249) or the lipid bilayer (W251 and R252) in the inactive state of the receptor (Figure 11). These observations strongly suggest that the cytoplasmic end of TM V does not undergo a major activity-dependent conformational change, such as a rotational movement or a partial unraveling of the helical structure, as proposed for the corresponding region of TM VI (see the discussion above).

Whereas agonist-induced structural changes have been studied in some detail in class I GPCRs, little is known about the molecular nature of the receptor conformations induced or stabilized by inverse agonists. Inverse agonists are defined as drugs that can reduce basal receptor activity or suppress signaling by constitutively active mutant GPCRs (*47–49*). Fluorescence-based studies with different adrenergic receptor subtypes suggest that inverse adrenergic agonists induce structural changes in their target receptors that differ in character and kinetics from those caused by agonist ligands (*29, 31*).

In the present study, we therefore also investigated whether treatment of the double Cys mutant $M_3$ receptors with atropine or NMS, two inverse muscarinic agonists (*45, 46*), had any effects on disulfide bond formation. These agents, traditionally considered prototypic muscarinic antagonists, have been reclassified as inverse muscarinic agonists based on their ability to reduce basal muscarinic receptor activity and inhibit signaling by constitutively active mutant muscarinic receptors (*45, 46*).

We found that atropine and NMS inhibited basal disulfide cross-linking displayed by the I253C/A489C, I253C/T491C, and I253C/L492C double Cys mutant receptors. As discussed above, muscarinic agonists facilitated disulfide bond formation in these three receptors. This observation strongly suggests that inverse muscarinic agonists, in contrast to muscarinic agonists, stabilize a receptor conformation characterized by reduced mobility of the cytoplasmic end of TM VI, associated with an increase in the distance between I253 (TM V) and this portion of TM VI.

In a recent disulfide cross-linking study (*28*), we demonstrated that inverse muscarinic agonists, in contrast to full muscarinic agonists, trigger a conformational change in the $M_3$ muscarinic receptor that reduces the distance between the N-terminal segment of the cytoplasmic tail (helix 8) and the cytoplasmic end of TM I. When these studies are taken together, they provide a structural basis for the opposing biological effects of muscarinic agonists and inverse agonists, highlighting the usefulness of disulfide cross-linking approaches to study changes in GPCR structure caused by different classes of agonist ligands.

Surprisingly, inverse agonists (atropine and NMS), similar to full muscarinic agonists (carbachol and acetylcholine), led to enhanced disulfide cross-linking in the Y250C/T491C and Y250C/L492C receptors. Whereas Y250 (TM V) directly faces L492 on TM VI, T491 lies on the opposite side of TM VI (Figure 11), projecting toward TM VII in the inactive state of the receptor. These observations suggest that inverse agonists, such as full agonists, may be able to cause local structural perturbations in the TM VI segment containing T491 and L492. These data also support the concept that full and inverse muscarinic agonists induce distinct structural changes in $M_3$ receptor structure that are not simply opposite each other.

Functional assays (measurements of basal IP levels) showed that both atropine and NMS suppressed basal IP accumulation in COS-7 cells expressing the M3′(3C)-Xa background receptor and the constitutively active I253C/Q490C mutant receptor, indicating that both ligands act as inverse agonists at these receptors. On the other hand, atropine and NMS had no significant effect on basal IP levels in the Y250C/T491C, Y250C/L492C, I253C/A489C, I253C/T491C, and I253C/L492C receptors. In most cases, however, we noticed at trend toward reduced basal signaling in samples incubated with atropine or NMS. In the absence of ligands, basal signaling was significantly reduced in the Y250C/T491C, Y250C/L492C, I253C/A489C, I253C/T491C, and I253C/L492C receptors (as compared to the M3′(3C)-Xa construct), most likely because of mutational modification of receptor domains known to be critically involved in receptor/G protein coupling (*21–23*). The reduced basal activity of these mutant receptors probably explains why atropine and NMS failed to show significant inverse activity at these receptors.

A comparison of the data given in Tables 1 and 2 revealed significant differences between carbachol $EC_{50}$ values measured in the disulfide cross-linking studies and carbachol affinities determined in radioligand-binding studies. The disulfide cross-linking reactions were carried out for only 10 min, whereas the carbachol-binding studies involved a 2 h incubation. One possibility therefore is that the disulfide cross-linking reactions, in contrast to the radioligand-binding studies, were carried out under nonequilibrium conditions, offering a possible explanation for the observed differences between carbachol $EC_{50}$ values and carbachol-binding affinities.

In summary, using a disulfide cross-linking strategy, we demonstrated that muscarinic agonists and inverse muscarinic agonists had different effects on the efficiency of disulfide bond formation in specific double Cys mutant $M_3$ receptors. Our data suggest that $M_3$ receptor activation does not trigger a major structural change within the cytoplasmic segment of TM V, in contrast to the adjacent region of TM VI. Together with a recent report (*28*), the present study also provides novel information about how the receptor conformations induced (or stabilized) by full versus inverse muscarinic agonists differ from each other at the structural level. Class I GPCRs are known to share a considerable degree of structural homology, which is particularly high among receptors activated by biogenic amine ligands. The conclusions drawn from the present study should therefore be applicable to many other members of the class I GPCR family.

## ACKNOWLEDGMENT

We thank Ms. Lanh Bloodworth for excellent technical support.

## REFERENCES

1. Bockaert, J., and Pin, J. P. (1999) Molecular tinkering of G protein-coupled receptors: An evolutionary success. *EMBO J. 18*, 1723–1729.

2. Gether, U. (2000) Uncovering molecular mechanisms involved in activation of G protein-coupled receptors. *Endocr. Rev. 21*, 90–113.
3. Pierce, K. L., Premont, R. T., and Lefkowitz, R. J. (2002) Seven-transmembrane receptors. *Nat. Rev. Mol. Cell. Biol. 3*, 639–650.
4. Kristiansen, K. (2004) Molecular mechanisms of ligand binding, signaling, and regulation within the superfamily of G-protein-coupled receptors: Molecular modeling and mutagenesis approaches to receptor structure and function. *Pharmacol. Ther. 103*, 21–80.
5. Foord, S. M., Bonner, T. I., Neubig, R. R., Rosser, E. M., Pin, J. P., Davenport, A. P., Spedding, M., and Harmar, A. J. (2005) International Union of Pharmacology. XLVI. G protein-coupled receptor list. *Pharmacol. Rev. 57*, 279–288.
6. Wess, J. (1998) Molecular basis of receptor/G-protein-coupling selectivity. *Pharmacol. Ther. 80*, 231–264.
7. Hubbell, W. L., Altenbach, C., Hubbell, C. M., and Khorana, H. G. (2003) Rhodopsin structure, dynamics, and activation: A perspective from crystallography, site-directed spin labeling, sulfhydryl reactivity, and disulfide cross-linking. *Adv. Protein Chem. 63*, 243–290.
8. Farrens, D. L., Altenbach, C., Yang, K., Hubbell, W. L., and Khorana, H. G. (1996) Requirement of rigid-body motion of transmembrane helices for light activation of rhodopsin. *Science 274*, 768–770.
9. Sheikh, S. P., Zvyaga, T. A., Lichtarge, O., Sakmar, T. P., and Bourne, H. R. (1996) Rhodopsin activation blocked by metal-ion-binding sites linking transmembrane helices C and F. *Nature 383*, 347–350.
10. Meng, E. C., and Bourne, H. R. (2001) Receptor activation: What does the rhodopsin structure tell us? *Trends. Pharmacol. Sci. 22*, 587–593.
11. Sakmar, T. P., Menon, S. T., Marin, E. P., and Awad, E. S. (2002) Rhodopsin: Insights from recent structural studies. *Annu. Rev. Biophys. Biomol. Struct. 31*, 443–484.
12. Palczewski, K., Kumasaka, T., Hori, T., Behnke, C. A., Motoshima, H., Fox, B. A., Le Trong, I., Teller, D. C., Okada, T., Stenkamp, R. E., Yamamoto, M., and Miyano, M. (2000) Crystal structure of rhodopsin: A G protein-coupled receptor. *Science 289*, 739–745.
13. Li, J., Edwards, P. C., Burghammer, M., Villa, C., and Schertler, G. F. (2004) Structure of bovine rhodopsin in a trigonal crystal form. *J. Mol. Biol. 343*, 1409–1438.
14. Gether, U., Lin, S., Ghanouni, P., Ballesteros, J. A., Weinstein, H., and Kobilka, B. K. (1997) Agonists induce conformational changes in transmembrane domains III and VI of the $\beta_2$ adrenoceptor. *EMBO J. 16*, 6737–6747.
15. Javitch, J. A., Fu, D., Liapakis, G., and Chen, J. (1997) Constitutive activation of the $\beta_2$ adrenergic receptor alters the orientation of its sixth membrane-spanning segment. *J. Biol. Chem. 272*, 18546–18549.
16. Rasmussen, S. G., Jensen, A. D., Liapakis, G., Ghanouni, P., Javitch, J. A., and Gether, U. (1999) Mutation of a highly conserved aspartic acid in the $\beta_2$ adrenergic receptor: Constitutive activation, structural instability, and conformational rearrangement of transmembrane segment 6. *Mol. Pharmacol. 56*, 175–184.
17. Sheikh, S. P., Vilardarga, J.-P., Baranski, T. J., Lichtarge, O., Iiri, T., Meng, E. C., Nissenson, R. A., and Bourne, H. R. (1999) Similar structures and shared switch mechanisms of the $\beta_2$-adrenoceptor and the parathyroid hormone receptor. Zn(II) bridges between helices III and VI block activation. *J. Biol. Chem. 274*, 17033–17041.
18. Jensen, A. D., Guarnieri, F., Rasmussen, S. G., Asmar, F., Ballesteros, J. A., and Gether, U. (2001) Agonist-induced conformational changes at the cytoplasmic side of transmembrane segment 6 in the $\beta_2$ adrenergic receptor mapped by site-selective fluorescent labeling. *J. Biol. Chem. 276*, 9279–9290.
19. Ward, S. D., Hamdan, F. F., Bloodworth, L. M., and Wess, J. (2002) Use of an *in situ* disulfide cross-linking strategy to map proximities between amino acid residues in transmembrane domains I and VII of the $M_3$ muscarinic acetylcholine receptor. *J. Biol. Chem. 277*, 2247–2257.
20. Ward, S. D., Hamdan, F. F., Bloodworth, L. M., Siddiqui, N. A., Li, J. H., and Wess, J. (2006) Use of an in situ disulfide cross-linking strategy to study the dynamic properties of the cytoplasmic end of transmembrane domain VI of the M3 muscarinic acetylcholine receptor. *Biochemistry 45*, 676–685.
21. Burstein, E. S., Spalding, T. A., Hill-Eubanks, D., and Brann, M. R. (1995) Structure−function of muscarinic receptor coupling to G proteins: Random saturation mutagenesis identifies a critical determinant of receptor affinity for G proteins. *J. Biol. Chem. 270*, 3141–3146.
22. Burstein, E. S., Spalding, T. A., and Brann, M. R. (1996) Amino acid side chains that define muscarinic receptor/G-protein coupling: Studies of the third intracellular loop. *J. Biol. Chem. 271*, 2882–2885.
23. Wess, J. (1996) Molecular biology of muscarinic acetylcholine receptors. *Crit. Rev. Neurobiol. 10*, 69–99.
24. Hulme, E. C., Birdsall, N. J., and Buckley, N. J. (1990) Muscarinic receptor subtypes. *Annu. Rev. Pharmacol. Toxicol. 30*, 633–673.
25. Hamdan, F. F., Ward, S. D., Siddiqui, N. A., Bloodworth, L. M., and Wess, J. (2002) Use of an *in situ* disulfide cross-linking strategy to map proximities between amino acid residues in transmembrane domains I and VII of the $M_3$ muscarinic acetylcholine receptor. *Biochemistry 41*, 7647–7658.
26. Han, S. J., Hamdan, F. F., Kim, S. K., Jacobson, K. A., Brichta, L., Bloodworth, L. M., Li, J. H., and Wess, J. (2005) Pronounced conformational changes following agonist activation of the $M_3$ muscarinic acetylcholine receptor. *J. Biol. Chem. 280*, 24870–24879.
27. Han, S. J., Hamdan, F. F., Kim, S. K., Jacobson, K. A., Bloodworth, L. M., Li, B., and Wess, J. (2005) Identification of an agonist-induced conformational change occurring adjacent to the ligand-binding pocket of the $M_3$ muscarinic acetylcholine receptor. *J. Biol. Chem. 280*, 34849–34858.
28. Li, J. H., Han, S. J., Hamdan, F. F., Kim, S. K., Jacobson, K. A., Bloodworth, L. M., Zhang, X., and Wess, J. (2007) Distinct structural changes in a G protein-coupled receptor caused by different classes of agonist ligands. *J. Biol. Chem. 282*, 26284–26293.
29. Gether, U., Lin, S., and Kobilka, B. K. (1995) Fluorescent labeling of purified $\beta_2$ adrenergic receptor. Evidence for ligand-specific conformational changes. *J. Biol. Chem. 270*, 28268–28275.
30. Ghanouni, P., Gryczynski, Z., Steenhuis, J. J., Lee, T. W., Farrens, D. L., Lakowicz, J. R., and Kobilka, B. K. (2001) Functionally different agonists induce distinct conformations in the G protein coupling domain of the $\beta_2$ adrenergic receptor. *J. Biol. Chem. 276*, 24433–24436.
31. Vilardaga, J. P., Steinmeyer, R., Harms, G. S., and Lohse, M. J. (2005) Molecular basis of inverse agonism in a G protein-coupled receptor. *Nat. Chem. Biol. 1*, 25–28.
32. Swaminath, G., Deupi, X., Lee, T. W., Zhu, W., Thian, F. S., Kobilka, T. S., and Kobilka, B. (2005) Probing the $\beta_2$ adrenoceptor binding site with catechol reveals differences in binding and activation by agonists and partial agonists. *J. Biol. Chem. 280*, 22165–22171.
33. Yao, X., Parnot, C., Deupi, X., Ratnala, V. R. P., Swaminath, G., Farrens, F., and Kobilka, B. (2006) Coupling ligand structure to specific conformational switches in the bold $\beta_2$-adrenoceptor. *Nat. Chem. Biol. 2*, 417–422.
34. Nikolaev, V. O., Hoffmann, C., Bünemann, M., Lohse, M. J., and Vilardaga, J. P. (2006) Molecular basis of partial agonism at the neurotransmitter $\alpha_{2A}$-adrenergic receptor and $G_i$-protein heterotrimer. *J. Biol. Chem. 281*, 24506–24511.
35. Granier, S., Kim, S., Shafer, A. M., Ratnala, V. R., Fung, J. J., Zare, R. N., and Kobilka, B. (2007) Structure and conformational changes in the C-terminal domain of the $\beta_2$-adrenoceptor: Insights from fluorescence resonance energy transfer studies. *J. Biol. Chem. 282*, 13895–13905.
36. Kobashi, K. (1968) Catalytic oxidation of sulfhydryl groups by *o*-phenanthroline copper complex. *Biochim. Biophys. Acta 158*, 239–245.
37. Zeng, F. Y., Hopp, A., Soldner, A., and Wess, J. (1999) Use of a disulfide cross-linking strategy to study muscarinic receptor structure and mechanisms of activation. *J. Biol. Chem. 274*, 16629–16640.
38. Zeng, F. Y., Soldner, A., Schöneberg, T., and Wess, J. (1999) Conserved extracellular cysteine pair in the $M_3$ muscarinic acetylcholine receptor is essential for proper receptor cell surface localization but not for G protein coupling. *J. Neurochem. 72*, 2404–2414.
39. Hulme, E. C., Lu, Z. L., and Bee, M. S. (2003) Scanning mutagenesis studies of the $M_1$ muscarinic acetylcholine receptor. *Recept. Channels 9*, 215–228.
40. Schmidt, C., Li, B., Bloodworth, L., Erlenbach, I., Zeng, F. Y., and Wess, J. (2003) Random mutagenesis of the $M_3$ muscarinic acetylcholine receptor expressed in yeast: Identification of point mutations that "silence" a constitutively active mutant $M_3$ receptor

and greatly impair receptor/G protein coupling. *J. Biol. Chem. 278*, 30248–30260.
41. Angers, S., Salahpour, A., and Bouvier, M. (2002) Dimerization: An emerging concept for G protein-coupled receptor ontogeny and function. *Annu. Rev. Pharmacol. Toxicol. 42*, 409–435.
42. George, S. R., O'Dowd, B. F., and Lee, S. P. (2002) G-protein-coupled receptor oligomerization and its potential for drug discovery. *Nat. Rev. Drug Discovery 1*, 808–820.
43. Zeng, F. Y., and Wess, J. (1999) Identification and molecular characterization of $M_3$ muscarinic receptor dimers. *J. Biol. Chem. 274*, 19487–19497.
44. Goin, J. C., and Nathanson, N. M. (2006) Quantitative analysis of muscarinic acetylcholine receptor homo- and heterodimerization in live cells: Regulation of receptor down-regulation by heterodimerization. *J. Biol. Chem. 281*, 5416–5425.
45. Spalding, T. A., Burstein, E. S., Brauner-Osborne, H., Hill-Eubanks, D., and Brann, M. R. (1995) Pharmacology of a constitutively active muscarinic receptor generated by random mutagenesis. *J. Pharmacol. Exp. Ther. 275*, 1274–1279.
46. Nelson, C. P., Nahorski, S. R., and Challiss, R. A. (2006) Constitutive activity and inverse agonism at the $M_2$ muscarinic acetylcholine receptor. *J. Pharmacol. Exp. Ther. 316*, 279–288.
47. Kenakin, T. (2001) Inverse, protean, and ligand-selective agonism: Matters of receptor conformation. *FASEB J. 15*, 598–611.
48. Strange, P. G. (2002) Mechanisms of inverse agonism at G-protein-coupled receptors. *Trends Pharmacol. Sci. 23*, 89–95.
49. Milligan, G. (2003) Constitutive activity and inverse agonists of G protein-coupled receptors: A current perspective. *Mol. Pharmacol. 64*, 1271–1276.
50. Bonner, T. I., Buckley, N. J., Young, A. C., and Brann, M. R. (1987) Identification of a family of muscarinic acetylcholine receptor genes. *Science 237*, 527–532.
51. Ballesteros, J. A., and Weinstein, H. (1995) Integrated methods for modeling G-protein coupled receptors. *Methods Neurosci. 25*, 366–428.

BI7019113